

Development of a triple-scale analysis method for plain-woven laminates based on a homogenization theory for time-dependent composites

Kohei Oide¹, *Tetsuya Matsuda¹, and Fumiya Kawasaki²

¹Department of Engineering Mechanics and Energy, University of Tsukuba
1-1-1 Tennoudai, Tsukuba, 305-8573, Japan

²All Nippon Airways Co. Ltd., Tokyo, 105-7133, Japan

*Corresponding author: matsuda@kz.tsukuba.ac.jp

Abstract

In this study, a triple-scale elastic-viscoplastic analysis method for plain-woven laminates is newly developed based on a homogenization theory for time-dependent composites. For this, triple-scale modeling of plain-woven laminates is performed by considering a plain-woven laminate as a macrostructure, plain fabrics and a matrix in the laminate as a mesostructure, and fibers and a matrix in the plain fabrics as a microstructure. Then, the boundary value problems for macro/meso and meso/micro scales are derived based on the homogenization theory for time-dependent composites, and the relationship between these problems are discussed. Using the relationship, a triple-scale elastic-viscoplastic analysis method for plain-woven laminates and its computational procedure are developed. It is shown that the present method is successful in taking into account the effects of elastoviscoplasticity of an epoxy matrix in plain fabrics on the elastic-viscoplastic behavior of plain-woven GFRP laminates.

Keywords: Plain-woven laminate, Triple-scale analysis, Homogenization, Viscoplasticity

Introduction

Plain-woven laminates made of plain fabrics and polymer materials are now regarded as some of the most important engineering materials, because of their high specific strength, high specific stiffness and good formability. Thus, they are used in major industrial fields such as aerospace, transportation and energy-related industries. It is therefore of great importance to clarify their mechanical properties.

The mathematical homogenization theory (Sanchez-Palencia, 1980) is one of the most useful theories for inelastic analysis such as damage analysis and elastic-viscoplastic analysis of plain-woven laminates. Thus, some researchers have already applied this theory to such analysis, and shown its usefulness. Takano et al. (1995) conducted a microscopic damage analysis of plain-woven glass fiber-reinforced plastic (GFRP) laminates. The authors (Matsuda et al., 2007; Matsuda et al., 2011) have performed the elastic-viscoplastic analysis of plain-woven GFRP laminates using

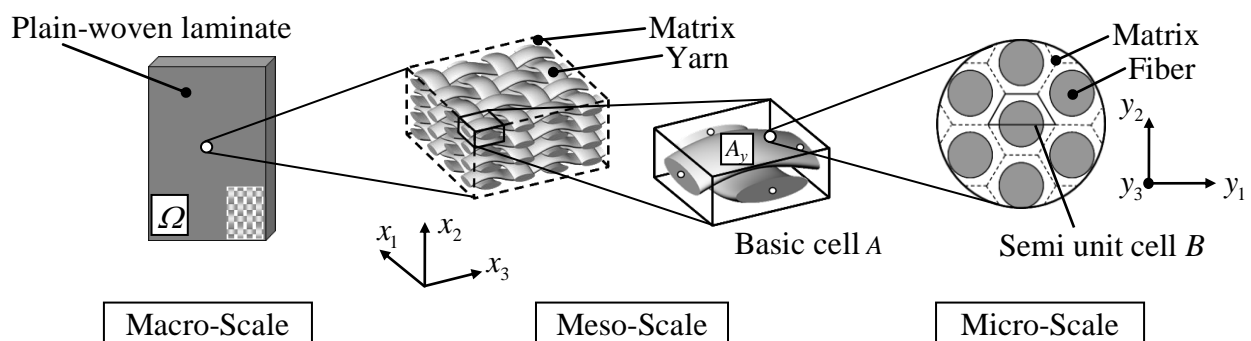


Figure 1. Triple-scale model of plain-woven laminates

the homogenization theory for nonlinear time-dependent composites (Wu and Ohno, 1991; Ohno et al., 2000). However, these studies regarded fiber bundles (yarns) in plain-woven laminates as homogeneous elastic materials, neglecting their microstructures consisting of fibers and matrix materials. In reality, yarns should exhibit not only elastic but also viscoplastic behavior due to the viscoplasticity of matrix materials. Therefore, to perform more advanced analysis of plain-woven laminates, it is necessary to develop a novel analysis method that is able to consider microstructures in yarns.

In this study, a triple-scale analysis method for plain-woven laminates which can consider viscoplasticity in yarns is newly developed based on the homogenization theory for time-dependent composites (Wu and Ohno, 1991; Ohno et al., 2000). First, plain-woven laminates are modeled in three scales as illustrated in Figure 1. Then, the homogenization theory for time-dependent composites is dually applied to the macro/meso and meso/micro problems, deriving an elastic-viscoplastic constitutive equation of the plain-woven laminates incorporating the microscopic information in yarns. Using the present theory, the elastic-viscoplastic analysis of plain-woven glass fiber/epoxy laminates is performed. Moreover, the results of analysis are compared with experimental data (Matsuda et al., 2007) to validate the analysis method.

Triple-Scale modeling of plain-woven laminates

Let us consider a plain-woven laminate Ω with microscopic periodic structure subjected to a macroscopic uniform load as illustrated in Figure 1. Then, a basic cell A consisting of yarns and a matrix is defined as a smallest unit in the meso-scale. Cartesian coordinates $x_i (i=1,2,3)$ are provided for the meso-scale. Next, in the micro-scale, a semiunit cell B consisting of a fiber and a matrix is defined as a smallest unit for the yarn region A_y in the basic cell A . Cartesian coordinates $y_i (i=1,2,3)$ are provided for the micro-scale. It is noted that the superscripts 0, 1 and 2 respectively indicate macro, meso and micro variables hereafter.

Micro/meso problem

Microscopic stress rate and strain rate fields in the semiunit cell B are denoted as ${}^2\dot{\sigma}_{ij}(\mathbf{y}, t)$ and ${}^2\dot{\epsilon}_{ij}(\mathbf{y}, t)$, respectively, where t represents time and $(\dot{})$ indicates differentiation with respect to t . Then, denoting partial differentiation with respect to y_i as $()_{,y_i}$, the equilibrium of microscopic stress is expressed as

$${}^2\dot{\sigma}_{ij,y_j} = 0. \quad (1)$$

The microscopic constitutive equation of each constituent in yarns is defined as

$${}^2\dot{\sigma}_{ij} = {}^2c_{ijkl}({}^2\dot{\epsilon}_{kl} - {}^2\beta_{kl}), \quad (2)$$

where ${}^2c_{ijkl}$ and ${}^2\beta_{kl}$ respectively represent the elastic stiffness and viscoplastic strain rate of fibers and a matrix, i.e.

$$\begin{aligned} {}^2c_{ijkl} &= c_{ijkl}^f \text{ or } c_{ijkl}^m & (f : \text{fiber}, m : \text{matrix}). \\ {}^2\beta_{kl} &= \beta_{kl}^f \text{ or } \beta_{kl}^m \end{aligned} \quad (3)$$

The microscopic velocity field ${}^2\dot{u}_i(\mathbf{y}, t)$ in B has the following expression:

$${}^2\dot{u}_i(\mathbf{y}, t) = {}^1\dot{F}_{ij}(\mathbf{x}, t)y_j + {}^2\dot{u}_i^\#(\mathbf{y}, t), \quad (4)$$

where ${}^1\dot{F}_{ij}(\mathbf{x}, t)$ denotes the mesoscopic deformation gradient, and ${}^2\dot{u}_i^\#(\mathbf{y}, t)$ denotes the microscopic perturbed velocity.

Now, let ${}^2v_i(\mathbf{y}, t)$ be an arbitrary variation of ${}^2\dot{u}_i^\#$ defined in B at t . Then, integration by parts and the divergence theorem allow Eq. (1) to be transformed to

$$\int_B {}^2\dot{\sigma}_{ij} {}^2v_{i,y_j} dB - \int_{\Gamma_B} {}^2\dot{\sigma}_{ij} n_j {}^2v_i d\Gamma_B = 0, \quad (5)$$

where Γ_B denotes the boundary of B , and n_j indicates the unit vector outward normal to Γ_B . In the above equation, the second term of the left-hand side, i.e. the boundary integral term, vanishes by considering the Y -periodicity and point-symmetry (Ohno et al., 2001) of ${}^2\dot{\sigma}_{ij}$ and 2v_i on Γ_B . Consequently, the second term of left-hand side in Eq. (5) vanishes, resulting in

$$\int_B {}^2\dot{\sigma}_{ij} {}^2v_{i,y_j} dB = 0. \quad (6)$$

By substituting Eq. (2) into Eq. (6), the following boundary value problems are derived:

$$\int_B {}^2c_{ijpq} {}^2\chi_{p,y_q}^{kl} {}^2v_{i,y_j} dB = - \int_B {}^2c_{ijkl} {}^2v_{i,y_j} dB, \quad (7)$$

$$\int_B {}^2c_{ijpq} {}^2\varphi_{p,y_q} {}^2v_{i,y_j} dB = \int_B {}^2c_{ijkl} {}^2\beta_{kl} {}^2v_{i,y_j} dB, \quad (8)$$

where ${}^2\chi_i^{kl}$ and ${}^2\varphi_i$ are characteristic functions obtained by solving the boundary value problems Eqs. (7) and (8). Then, the evolution equation of microscopic stress rate ${}^2\dot{\sigma}_{ij}$ is expressed as

$${}^2\dot{\sigma}_{ij} = \left[{}^2c_{ijkl} (\delta_{pk} \delta_{ql} + {}^2\chi_{p,y_q}^{kl}) \right] {}^1\dot{\epsilon}_{kl} - \left[{}^2c_{ijkl} ({}^2\beta_{kl} - {}^2\varphi_{k,y_l}) \right], \quad (9)$$

where δ_{ij} indicates Kronecker's delta. Then, the relation between mesoscopic stress rate and strain rate is derived as follow:

$$\begin{aligned} {}^1\dot{\sigma}_{ij} &= {}^1c_{ijkl} ({}^1\dot{\epsilon}_{kl} - {}^1\beta_{kl}) \\ &= \left\langle {}^2c_{ijkl} (\delta_{ik} \delta_{jl} + {}^2\chi_{i,y_j}^{kl}) \right\rangle_B {}^1\dot{\epsilon}_{kl} - \left\langle {}^2c_{ijkl} ({}^2\beta_{kl} - {}^2\varphi_{k,y_l}) \right\rangle_B, \end{aligned} \quad (10)$$

where $\langle \cdot \rangle_B$ designates the volume average in B defined as $\langle \# \rangle_B = |B|^{-1} \int_B \# dB$, in which $|B|$ signifies the volume of B .

Meso/macro problem

Mesoscopic stress rate and strain rate fields in the basic cell A are denoted as ${}^1\dot{\sigma}_{ij}(\mathbf{x}, t)$ and ${}^1\dot{\epsilon}_{ij}(\mathbf{x}, t)$, respectively. Then, denoting partial differentiation with respect to x_i as $(\cdot)_{,x_i}$, the equilibrium of mesoscopic stress is expressed as

$${}^1\dot{\sigma}_{ij,x_j} = 0. \quad (11)$$

The mesoscopic constitutive equation of each constituent in the plain-woven laminate is defined as

$${}^1\dot{\sigma}_{ij} = {}^1c_{ijkl} ({}^1\dot{\epsilon}_{kl} - {}^1\beta_{kl}) = {}^1c_{ijkl} {}^1\dot{\epsilon}_{kl} - {}^1c_{ijkl} {}^1\beta_{kl}, \quad (12)$$

where ${}^1c_{ijkl}$ and ${}^1\beta_{kl}$ respectively represent the elastic stiffness and viscoplastic strain rate of yarns and a matrix in the plain-woven laminate, i.e.

$$\begin{aligned} {}^1c_{ijkl} &= c_{ijkl}^y \text{ or } c_{ijkl}^m \\ {}^1\beta_{kl} &= \beta_{kl}^y \text{ or } \beta_{kl}^m \end{aligned} \quad (y: \text{yarn}, m: \text{matrix}). \quad (13)$$

Here, comparing Eq. (10) with Eq. (12), the following relationships can be obtained:

$${}^1c_{ijkl} = c_{ijkl}^y = \left\langle {}^2c_{ijkl} \left(\delta_{ik} \delta_{jl} + {}^2\chi_{i,y_j}^{kl} \right) \right\rangle_B, \quad (14)$$

$${}^1c_{ijkl} {}^1\beta_{kl} = c_{ijkl}^y \beta_{kl}^y = \left\langle {}^2c_{ijkl} \left({}^2\beta_{kl} - {}^2\varphi_{k,y_l} \right) \right\rangle_B. \quad (15)$$

The mesoscopic velocity field ${}^1\dot{u}_i(\mathbf{x}, t)$ in A has the following expression:

$${}^1\dot{u}_i(\mathbf{x}, t) = {}^0\dot{F}_{ij}(t) x_j + {}^1\dot{u}_i^\#(\mathbf{x}, t), \quad (16)$$

where ${}^0\dot{F}_{ij}(t)$ denotes the macroscopic deformation gradient, and ${}^1\dot{u}_i^\#(\mathbf{x}, t)$ denotes the mesoscopic perturbed velocity, respectively.

Now, let ${}^1v_i(\mathbf{x}, t)$ be an arbitrary variation of ${}^1\dot{u}_i^\#$ defined in A at t . Then, considering Y -periodicity and point-symmetry (Ohno et al., 2001) of ${}^1\dot{\sigma}_{ij}$ and 1v_i on the boundary of basic cell A , Γ_A , the following equation is derived in the same manner as in the preceding section:

$$\int_A {}^1\dot{\sigma}_{ij} {}^1v_{i,x_j} dA = 0. \quad (17)$$

By substituting Eq. (12) into Eq. (17), the following boundary value problems are derived:

$$\int_A {}^1c_{ijpq} {}^1\chi_{p,x_q}^{kl} {}^1v_{i,x_j} dA = - \int_A {}^1c_{ijkl} {}^1v_{i,x_j} dA, \quad (18)$$

$$\int_A {}^1c_{ijpq} {}^1\varphi_{p,x_q} {}^1v_{i,x_j} dA = \int_A {}^1c_{ijkl} {}^1\beta_{kl} {}^1v_{i,x_j} dA, \quad (19)$$

where ${}^1\chi_i^{kl}$ and ${}^1\varphi_i$ are characteristic functions obtained by solving the boundary value problems Eqs. (18) and (19). Then, the evolution equation of mesoscopic stress rate ${}^1\dot{\sigma}_{ij}$ is expressed as

$${}^1\dot{\sigma}_{ij} = \left[{}^1c_{ijkl} \left(\delta_{pk} \delta_{ql} + {}^1\chi_{p,x_q}^{kl} \right) \right] {}^0\dot{\epsilon}_{kl} - \left[{}^1c_{ijkl} \left({}^1\beta_{kl} - {}^1\varphi_{k,x_l} \right) \right]. \quad (20)$$

Then, the relation between macroscopic stress rate and strain rate is derived as follows:

$$\begin{aligned} {}^0\dot{\sigma}_{ij} &= {}^0c_{ijkl} ({}^0\dot{\epsilon}_{kl} - {}^0\beta_{kl}) \\ &= \left\langle {}^1c_{ijkl} \left(\delta_{ik} \delta_{jl} + {}^1\chi_{i,x_j}^{kl} \right) \right\rangle_A {}^0\dot{\epsilon}_{kl} - \left\langle {}^1c_{ijkl} \left({}^1\beta_{kl} - {}^1\varphi_{k,x_l} \right) \right\rangle_A, \end{aligned} \quad (21)$$

where $\langle \cdot \rangle_A$ designates the volume average in A defined as $\langle \# \rangle_A = |A|^{-1} \int_A \# dA$, in which $|A|$ signifies the volume of A .

Using the Eqs. (20) and (21) accompanied by Eqs. (14) and (15), the elastic-viscoplastic behavior of plain-woven laminates can be analyzed through the triple scales.

Analysis conditions

In the present analysis, elastic-viscoplastic behavior of a plain-woven glass fiber/epoxy composite laminate manufactured by Nitto Shinko Corporation (10 plain fabrics stacked) was analyzed using the theory developed. A basic cell A was defined as shown in Figure 2 in accordance with the microscope observation (Matsuda et al., 2007) of the plain-woven GFRP laminate, and was divided into eight-node isoparametric elements (1624 elements, 1995 nodes). On the other hand, a semiunit cell B of yarns was defined as depicted in Figure 3, and was divided into four-node isoparametric elements assuming the generalized plain strain condition (81 elements, 97 nodes). For B , the fiber volume fraction was set to be 75% (Matsuda et al., 2007).

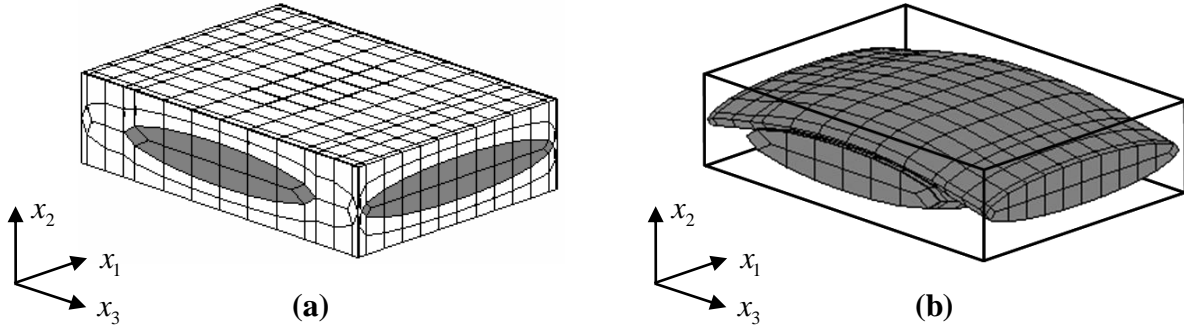


Figure 2. Basic cell A of the plain-woven laminate in meso-scale and finite element mesh: (a) full view and (b) yarns in basic cell

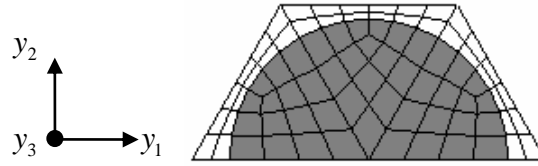


Figure 3. Semiunit cell B of the yarns in micro-scale and finite element mesh

Table 1. Material constants

Glass fiber	$E_f = 80.0$	$\nu_f = 0.30$
Epoxy	$E_m = 5.0$	$\nu_m = 0.35$
	$\dot{\epsilon}_0^p = 1.0 \times 10^{-5}$	
	$n = 25$	$g(\bar{\epsilon}^p) = 105.0(\bar{\epsilon}^p)^{0.20} + 24.5$
GPa(stress),mm/mm(strain),s(time)		

The plain-woven laminate was subjected to macroscopic uniaxial tension at a constant strain rate ${}^0\dot{\epsilon}_\theta = 10^{-5} \text{ [s}^{-1}\text{]}$ at room temperature. The loading directions were $0^\circ, 15^\circ, 30^\circ$ and 45° -directions rotated from the x_3 -direction in the $x_1 - x_3$ plane.

The material constants of fibers and an epoxy matrix are listed in Table 1. The glass fibers were regarded as isotropic elastic materials. The epoxy matrix, on the other hands, was regarded as an isotropic elastic-viscoplastic material which obeyed the following constitutive equation:

$$\dot{\epsilon}_{ij} = \frac{1+\nu_m}{E_m} \dot{\sigma}_{ij} - \frac{\nu_m}{E_m} \dot{\sigma}_{kk} \delta_{ij} + \frac{3}{2} \dot{\epsilon}_0^p \left[\frac{\sigma_{eq}}{g(\bar{\epsilon}^p)} \right]^n \frac{s_{ij}}{\sigma_{eq}}, \quad (22)$$

where E_m, ν_m, n signify the material constants, $g(\bar{\epsilon}^p)$ stands for a hardening function depending on equivalent viscoplastic strain $\bar{\epsilon}^p$, $\dot{\epsilon}_0^p$ indicates reference strain rate, s_{ij} denotes the deviatoric part of σ_{ij} , and $\sigma_{eq} = [(3/2)s_{ij}s_{ij}]^{1/2}$. Incidentally, no failure was assumed to occur in the glass fibers and an epoxy.

Results of analysis

Figure 4 shows the macroscopic stress-strain relations of the plain-woven GFRP laminate subjected to the uniaxial tension in the $0^\circ, 15^\circ, 30^\circ$ and 45° -directions. As seen from the experimental data,

the macroscopic stress-strain relations markedly vary depending on the loading direction. Thus, it can be said that the plain-woven GFRP laminate has remarkable elastic-viscoplastic anisotropy. Comparing such experimental data with the results of the present analysis indicated by the lines in Figure 4, it is found that the present method is successful in predicting the macroscopic behavior of the plain-woven GFRP laminate.

Figures 5-8 show the distributions of mesoscopic equivalent plastic strain in the basic cell *A*. As seen from Figure 5, very small plastic strain is observed in the yarns with the on-axis loading. In contrast, high plastic strain can be found with the off-axis loading as shown in Figures 6-8. It is emphasized that such plastic strain in yarns was not able to be considered in the previous studies.

Finally, Figure 9 shows the microscopic equivalent plastic strain distribution at the points (i) and (ii) in the yarn when $\theta = 45^\circ$. As seen from the figure, considerably large plastic strain occurs at the interface of the fiber and epoxy matrix in the semiunit cell *B*. This also cannot be dealt with in the previous studies.

Conclusions

In the present study, a triple-scale analysis method for plain-woven laminates was developed based on the homogenization theory for nonlinear time-dependent composites. Then, the elastic-viscoplastic behavior of a plain-woven glass fiber/epoxy laminate was analyzed using the present method. Moreover, the analysis results were compared with experimental data. The stress-strain curves in the macro-scale showed remarkable anisotropy, and the analysis results were in good agreement with the experimental data. From the equivalent plastic strain distribution in the meso-scale, considerable plastic strain was observed in yarns when the plain-woven GFRP laminate was subjected to off-axis tensile loading. It was also observed that, in the micro-scale, large equivalent plastic strain was accumulated at the epoxy matrix in yarns. It should be noted that these results cannot be obtained using the previous methods which completely neglected the viscoplasticity of yarns.

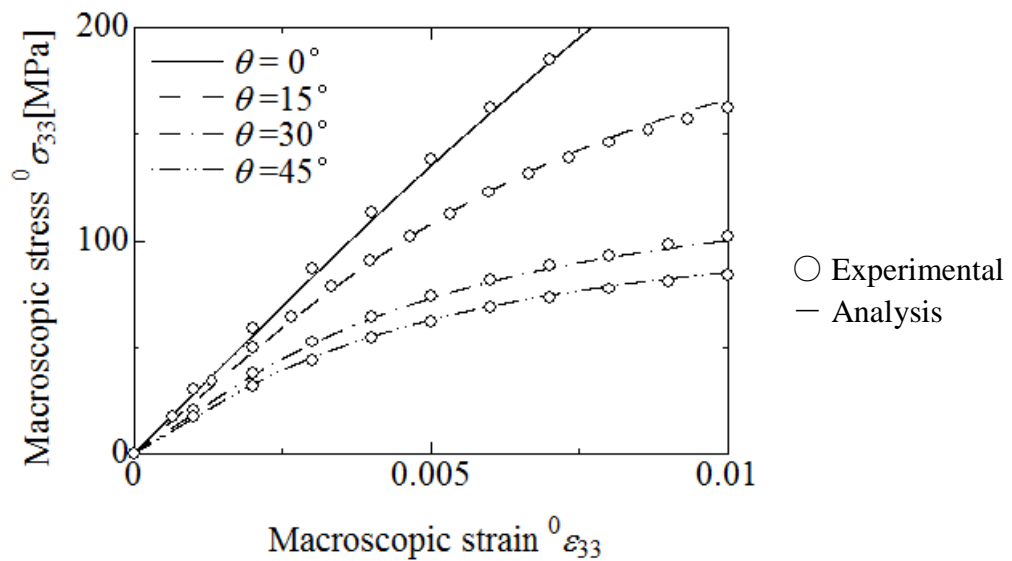


Figure 4. Macroscopic stress-strain relations

Reference

- Matsuda. T, Nimiya. Y, Ohno. N, and Tokuda. M (2007), Elastic-viscoplastic behavior of plain-woven GFRP laminates Homogenization using reduced domain of analysis, *Compos. Struct.*, 79, pp. 493-500.
- Matsuda. T, Kanamaru. S, Yamamoto. N, and Fukuda. Y (2011), A homogenization theory for elastic-viscoplastic materials with misaligned internal structures, *Int. J. Plast.*, 27, pp. 2056-2067.
- Ohno. N, Wu. X, Matsuda. T (2000), Homogenized properties of elastic-viscoplastic composites with periodic integral structures, *Int. J. Mech. Sci.*, pp. 1519-1536.
- Ohno. N, Matsuda. T, Wu. X (2001), A homogenization theory for elastic-viscoplastic composites with point symmetry of internal distributions, *Int. J. Solids Struct.*, 38, pp. 2867-2878.
- Sanchez-Palencia. E (1980), *Non-Homogeneous Media and Vibration Theory*, Lecture Notes in Physics, No. 127, Springer-Verlag, Berlin.
- Takano. N, Zako. M, Sakaki. S (1995), Three-dimensional microstructural design of woven fabric composite materials by the homogenization method: 1st report, effect of mismatched lay-up of woven fabrics on the strength, *Trens. Jpn Soc. Mech. Eng. Ser. A*, 61, pp.1038-1043.
- Wu. X, Ohno. N (1999), A homogenization theory for time-dependent nonlinear composites with periodic internal structures, *Int. J. Solids Struct.*, 36, pp.4991-5012.

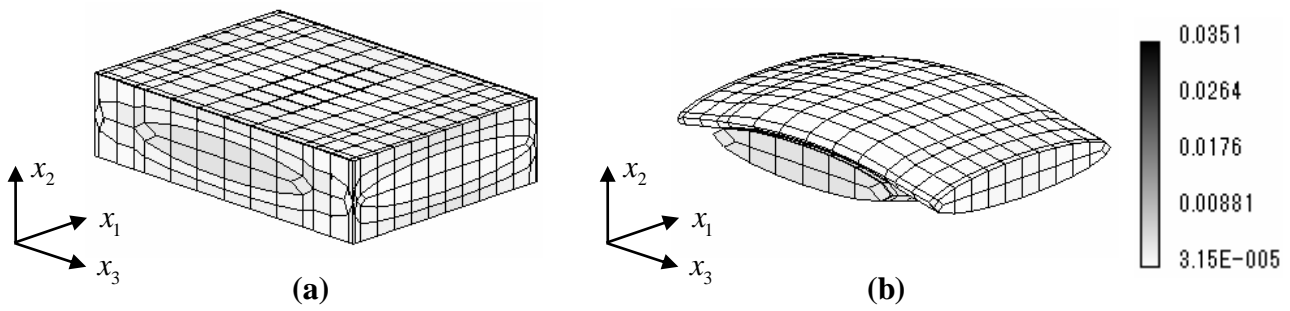


Figure 5. Mesoscopic equivalent plastic strain distribution ($\theta = 0^\circ$): (a) full view and (b) yarns

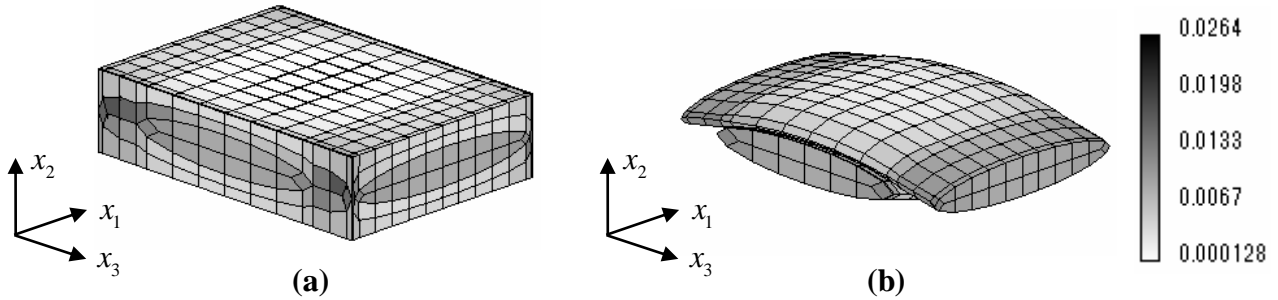


Figure 6. Mesoscopic equivalent plastic strain distribution ($\theta = 15^\circ$): (a) full view and (b) yarns

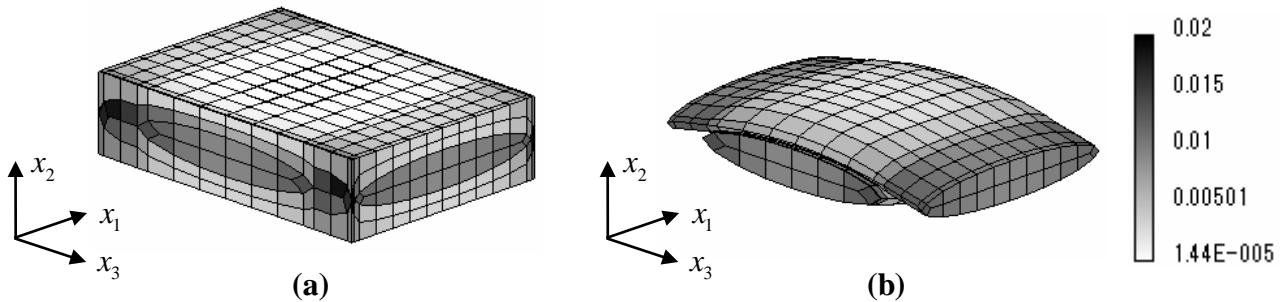


Figure 7. Mesoscopic equivalent plastic strain distribution ($\theta = 30^\circ$): (a) full view and (b) yarns

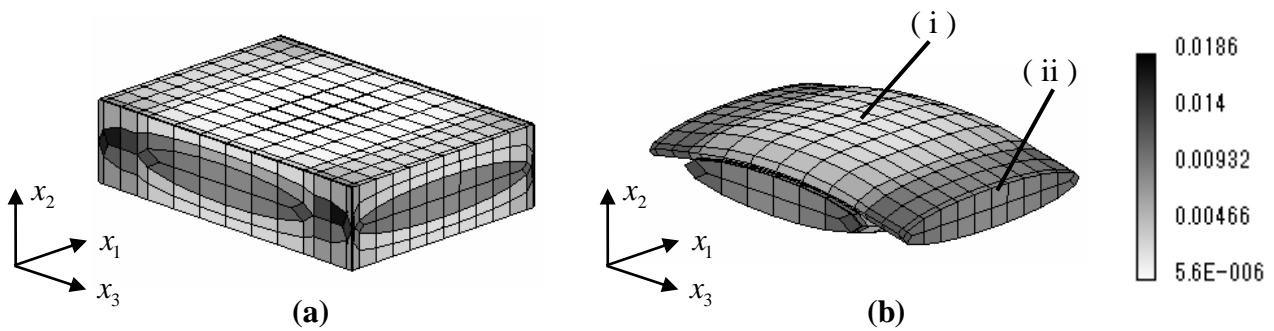


Figure 8. Mesoscopic equivalent plastic strain distribution ($\theta = 45^\circ$): (a) full view and (b) yarns

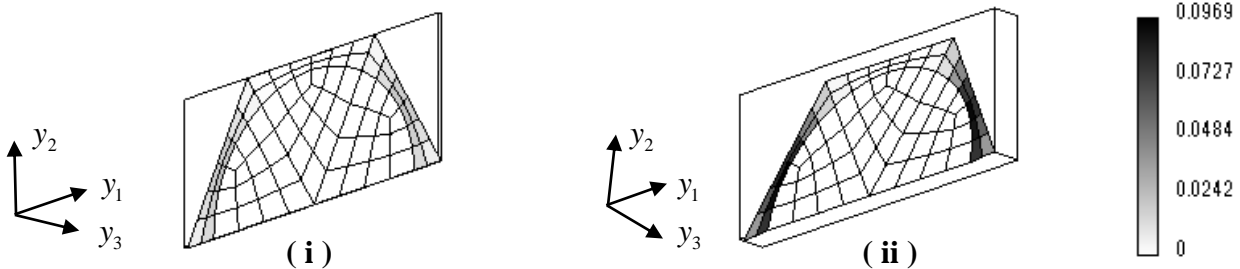


Figure 9. Microscopic equivalent plastic strain distribution at (i) and (ii)